Thermal Losses in a Coaxial Pulse Tube Cryocooler

H. Rana, M.A. Abolghasemi, R. Stone, M. Dadd, P. Bailey

Department of Engineering Science, University of Oxford
Oxford, OX1 3PJ United Kingdom

ABSTRACT

Conductive and radiative losses in pulse tube cryocoolers are difficult to predict, particularly in a coaxial configuration. The static losses in a pulse tube must be accounted for and factored when determining the cooling power and the thermal losses as a result of radiation must be quantified to establish their significance. Studies have previously shown that there is a discrepancy between computationally simulated cooling performances and experimentally measured values. This could be attributed to the under-prediction of thermal losses in numerical models. A lumped parameter model using ESATAN-TMS was created to determine the thermal losses in a coaxial pulse tube cryocooler in order to independently investigate the role the estimation of these losses may play in the discrepancy between experimental and computed values. The conductive losses simulated closely matched those determined by the Sage numerical model, and the radiative losses appear to be negligible. An analysis of an independent method for simulating thermal losses of a coaxial pulse tube and its impact on cooling performance is presented.

INTRODUCTION

Pulse tube cryocoolers provide active cooling for space instruments, superconducting devices, and other terrestrial equipment to cryogenic temperatures. The pulse tube cryocooler operates by running helium gas through thermodynamic cycles to achieve cooling at the cold head. This cooling depends on a well-designed interplay between the mass flow and pressure pulse within the pulse tube and regenerator [1]. Pulse tube cryocoolers are often designed in a coaxial configuration in order to reduce dead volume and enhance the ease of integration between the cooling interface and the cold head [2].

The thermal losses in the pulse tube cryocooler can be difficult to predict, especially when in a coaxial configuration, and should be quantified accurately as the losses affect the overall cooling performance and efficiency of the cryocooler. It is further important to ascertain the significance of any radiative losses of the system. Numerical models can be used to predict the performance of the pulse tube cryocooler. A coaxial Stirling pulse tube cryocooler (SPTC) with an active displacer was previously numerically studied [3] and experimentally investigated [4]. A discrepancy was observed between the experimentally measured performance and the numerically computed output. Some attempts were made to improve the model validation by tying certain regions to known measured temperatures from the experimental findings, in order to minimize the discrepancy. Given that it is difficult to fully replicate the complex coaxial geometry in the numerical Sage model, there is a possibility that the conductive losses are underestimated, thereby impacting the numerically simulated cryocooler performance. As such, it is of use to conduct an independent investigation of the conductive losses in the cryocooler and investigate the magnitude of any radiative losses.

Cryocoolers 21, edited by R.G. Ross, Jr., J.R. Raab and S.D. Miller

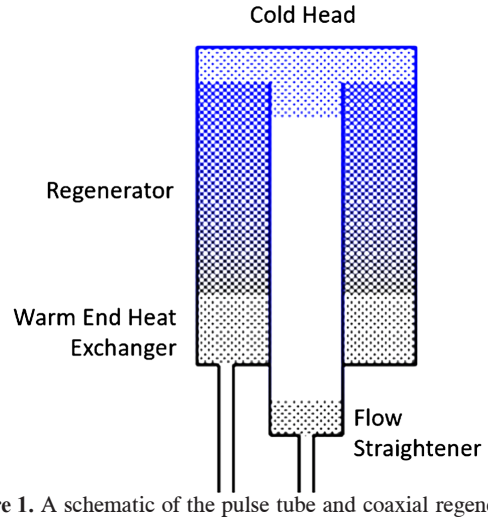

Figure 1. A schematic of the pulse tube and coaxial regenerator.

ESATAN-TMS was selected as a suitable software for modelling the thermal losses [5]. This permitted the creation of a lumped parameter model of the coaxial pulse tube in order to predict the thermal losses. The output from these simulations were then fed back into the existing numerical model to re-validate the experimental findings of cryocooler performance with the numerical simulation. This paper outlines the modelling methodology and findings of thermal losses, focusing on conductive and radiative thermal losses.

SPTC DESIGN & MODELLING

Coaxial pulse tube design

A schematic of the pulse tube in the coaxial arrangement is shown in Figure 1. The pulse tube is a 90 mm long G10 epoxy-glass tube fitted into the regenerator, which is a 60 mm long Stainless Steel 316 (SS316) tube with a wall thickness of 0.25 mm. Flow reversal occurs at the coaxial cold head and there is a flow straightener at either end of the pulse tube. The structure is surrounded by an aluminised Mylar radiation shield before being placed into the vacuum tank.

Numerical Model Validation

The performance of the SPTC with an active displacer is shown in Figure 2, indicating how the cooling power and relative Carnot efficiency changes with displacer phase (left) and stroke (right). In blue, the cooling power for both experimental data and the simulated performance (using Sage software) can be seen. The Sage model was improved by tying certain boundaries to temperatures measured during experiments. The discrepancy in the model validation is approximately 0.5 W when averaged across the sweeps in terms of cooling power, and an average of 4% difference in relative Carnot efficiency. This discrepancy could potentially be attributed to the underestimation in the numerical model of the conductive losses in the system. These can be difficult to model due to the complex coaxial geometry of the pulse tube and regenerator. These losses are critical as they transfer thermal energy from the warm end to the cold end, degrading the cooling performance. The Sage numerical model computes 0.65 W of conductive losses in the coaxial SPTC.

ESATAN-TMS software

ESATAN-TMS was the software identified for modelling the conductive and radiative losses of the cryocooler. The software is written in standard ANSI Fortran 77 and allows lumped parameter modelling.

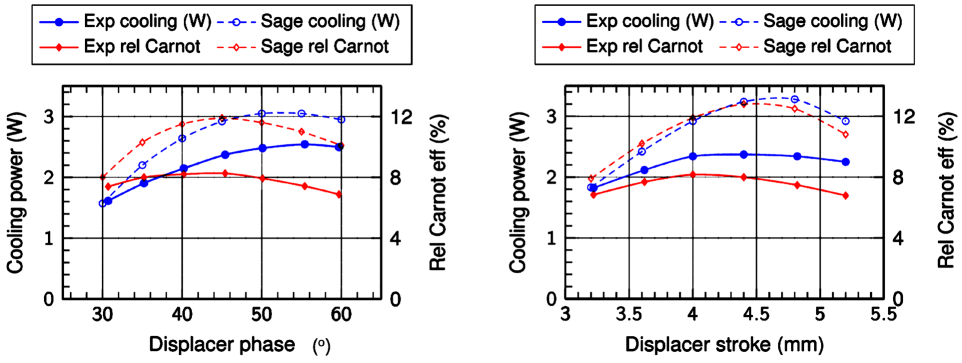

Figure 2. Change in cooling power and relative Carnot efficiency as displacer phase is varied (left) and displacer stroke is varied (right). The discrepancy between the Sage model output compared to the experimentally determined performance can be observed.

The prediction of temperature distributions can be achieved across modelled nodes, in which each are modelled to represent a key region in the pulse tube where the temperature is affected by significant heat transfer. The software does not permit convective modelling, however, and thus CFD and coupled multi-physics simulations will be required for this. Typical inputs that are applied to the nodes include thermal conductivity, specific heat capacity, and thermo-optical surface properties, such as emissivity and absorptivity.

Material Properties

The material properties of the surfaces used for the conductive and radiative model are shown in the Table 1 and Figure 3. As a key input affecting the output of the model, the material properties need to be as accurate as possible. Furthermore, the variation due to temperature, particularly over a wide range of 80-300 K, has to be accounted for. The following curve fitting equation for material properties was utilised to obtain values across the 80 K to 300 K temperature range in the pulse tube. The coefficients a-f, representing the material properties, are obtained from the NIST Cryogenic Material properties database [6]. The obtained distributions, shown in Figure 3 for thermal conductivity and specific heat capacity, are then fed into the model as temperature-dependent matrices.

$$\log_{10} y = a + b(\log_{10} T) + c(\log_{10} T)^2 + d(\log_{10} T)^3 + e(\log_{10} T)^4 + f(\log_{10} T)^5 \quad (1)$$

MODELLING AND ANALYSIS

Conductive losses

The conduction between nodes is calculated as shown in Equation 2, where Q is the heat flux (W), k is the thermal conductivity, A is the surface area, ΔT is the temperature difference between the two nodes, and l is the length. The linear conductance used in ESATAN-TMS that arises from thermal conductance is represented by GL, as given in Equation 3, which is the form of the output from the model.

$$Q = k\,A\,\Delta T / l \quad (2)$$

$$GL = k\,A / l \quad (3)$$

Table 1. The emissivity coefficients for the regenerator (SS316) and the pulse tube (G10).

Thermo-optical Surface	Emissivity, ε
Regenerator (SS316)	0.910
Pulse tube (G10)	0.350

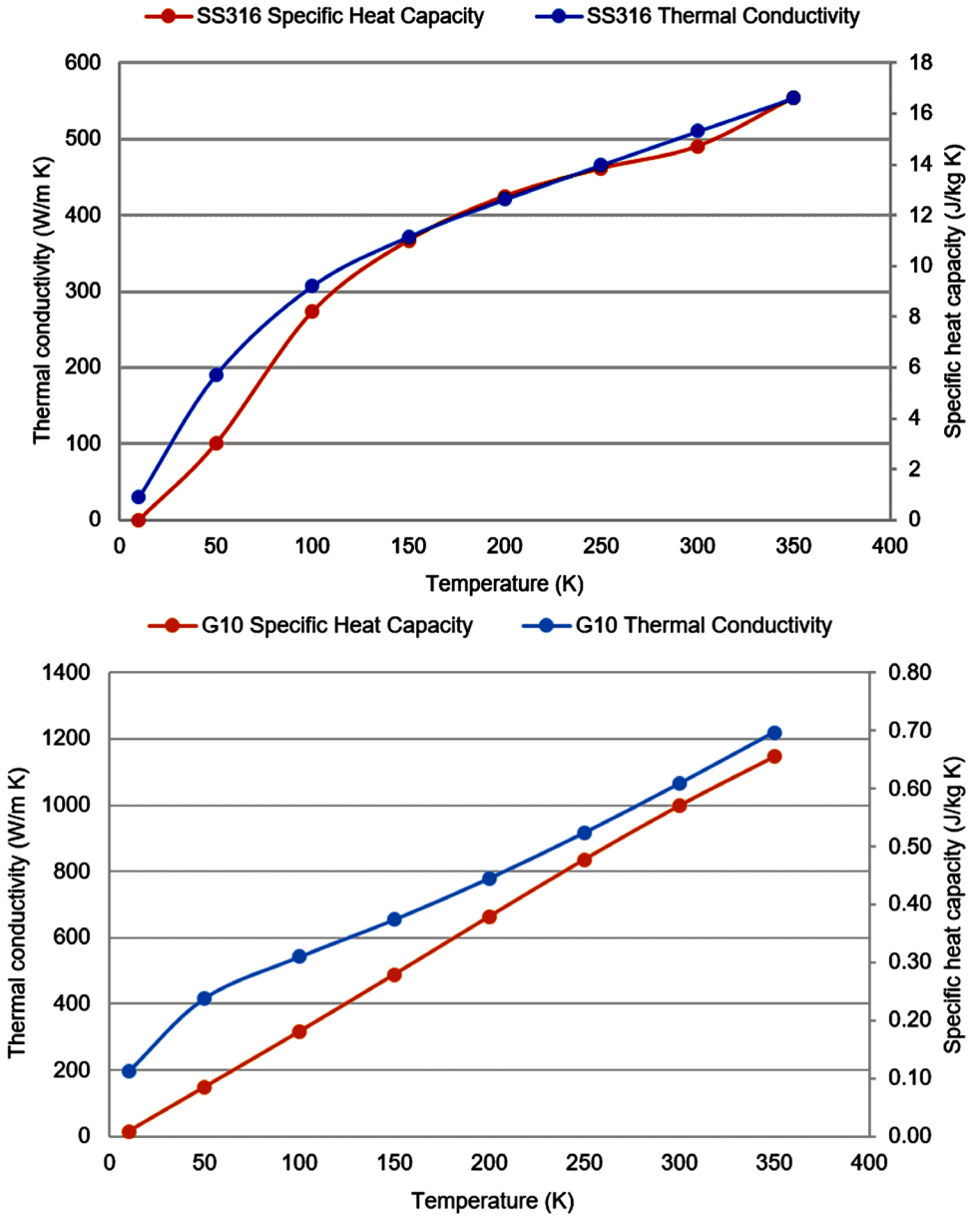

Figure 3. Thermal conductivity and specific heat capacity as a function of temperature for the SS316 regenerator (above) and the G10 pulse tube (below). These distributions were the material property inputs for both components, in addition to the parameters in Table 1**.**

The contact conductance is best determined experimentally for materials, as they are affected by factors such as surface finish, temperature, as well as the pressure applied at the contact. Figure 4 shows the user interface representation of the axi-symmetrical model of the regenerator and pulse tube. The coaxial regenerator is shown in green and the pulse tube in blue, and the sections indicate the different nodes modelled. The heat flow was computed both radially and axially. The simulated total conductive losses were found to be approximately 0.7 W. Table 2 shows the conduction output from the simulation.

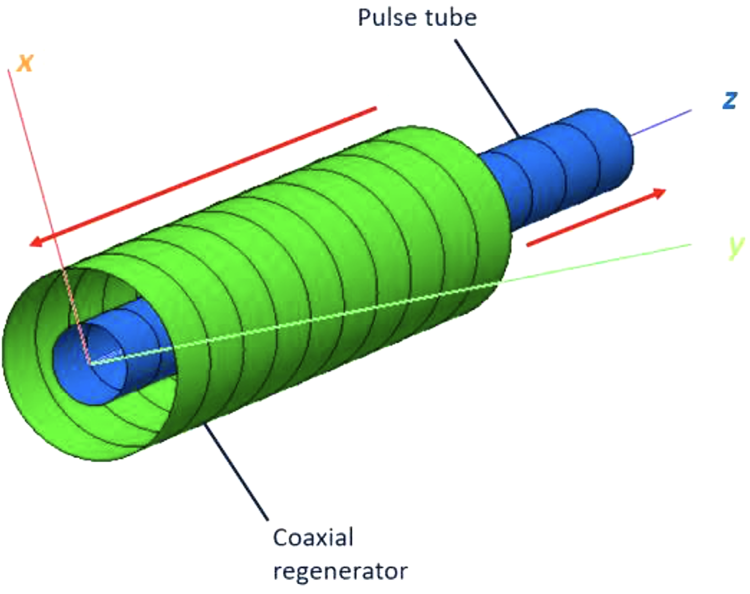

Figure 4. The coaxial regenerator (green) and the pulse tube (blue) modelled in ESATAN-TMS. The sections indicate the nodes modelled. The x, y, and z model axes are also shown. Note that this particular diagram solely depicts the surfaces.

Table 2. The *GL* output and the corresponding conduction calculated for the regenerator and the pulse tube in the coaxial arrangement shown in Figure 4.

Collective Nodes	GL (ESATAN) [W/K]	Conduction [W]
Regenerator	0.141	0.64
Pulse tube	0.00149	0.034

Radiative losses

The radiative losses from the pulse tube system required quantifying to ascertain their significance. ESATAN-TMS uses enhanced Monte-Carlo ray tracing algorithms to calculate view factors. This allows for rapid analysis of radiative heat exchange between surfaces. The *GR*, the radiative coupling between two surfaces 1 and 2, is given by Equation 4, and is the form the model output takes,

$$GR_{1,2} = \varepsilon \, \sigma \, A \, F_{1,2} \, (T_1^4 - T_2^4) \tag{4}$$

where ε the emissivity, σ is the Stefan-Boltzmann constant, A is the surface area, $F_{1,2}$ is the view factor between surfaces 1 and 2, and T the temperature.

Table 3 shows the calculated total radiative heat flux from the coaxial regenerator-pulse tube arrangement. The computed values are expectably low, and radiative heat flux from the G10 pulse tube was negligible.

Table 3. The calculated output for the radiative ray tracing model, as a result of computed GR values, between all node surfaces firstly from the regenerator to the pulse tube, and secondly, in the opposite direction.

Direction	Radiative heat flux [W]
Regenerator-PT	0.038
PT-Regenerator	Negligible

DISCUSSION AND NEXT STEPS

The conductive and radiative losses of the regenerator and the pulse in the SPTC were computed using ESATAN-TMS. The combined total thermal losses were found to be approximately 0.7 W, closely matching the value of 0.65 W computed by the Sage numerical model. The radiative losses from the coaxial regenerator and pulse tube arrangement were considerably lower. The discrepancy in the model validation is due to many factors and does not seem attributable to errors in the conduction loss calculations alone. Figure 2 indicates that the difference in performance is not consistent, rather, it changes with varying stroke and phase angle. This matter requires further investigation, where unaccounted dead volumes in the experimental setup may need to be matched up with the numerical model. In addition to this, further analysis would require a thermo-fluid model to assess any convective losses, particularly those due to flow mixing, to complete a holistic assessment of all thermal losses within the system.

ACKNOWLEDGMENTS

The authors would like to acknowledge partial funding from the EPSRC with EP/N017013/1 and Honeywell Hymatic for this project and broader SPTC research within the Cryogenic Engineering group at the University of Oxford. Furthermore, they would like to thank the reviewers of *Cryocoolers*.

REFERENCES

1. Radebaugh, R., "Development of the pulse tube refrigerator as an efficient and reliable cryocooler," *Proceedings of Institute of Refrigeration*, Vol. 96 (2000), pp. 11-29.
2. Dang, H., "40 K single-stage coaxial pulse tube cryocoolers," *Cryogenics*, Vol. 52 (2012), pp. 216-220.
3. Rana, H., et al., "Numerical modelling of a coaxial Stirling pulse tube cryocooler with an active displacer for space applications," *Cryogenics*, Vol. 106 (2020).
4. Abolghasemi, M.A. et al., "Coaxial Stirling pulse tube cryocooler with active displacer," *Cryogenics*, Vol. 111 (2020).
5. Fereday, J., et al., "Cryocooler modelling methodology," *Cryogenics*, Vol. 46 (2006), pp. 183-190.
6. NIST, "Cryogenic Material Properties database", Available at: https://trc.nist.gov/cryogenics/materials/materialproperties.htm. Accessed the 4th, December (2020).